

DOI: <https://doi.org/10.21123/bsj.2023.7763>

## Preparation and Characterization of Silver Nanoparticles and its Medical Application against Pathogenic Bacteria

Azhin Zainel Abbas <sup>1</sup> 

Rosure Borhanalden Abdulrahman <sup>1\*</sup> 

Thikra A. Mustafa <sup>2</sup> 

<sup>1</sup> Department of Physics, College of Science, University of Kirkuk, Kirkuk, Iraq.

<sup>2</sup> College of Veterinary Medicine, University of Kirkuk, Kirkuk, Iraq.

\*Corresponding author: [rbadulrahman@uokirkuk.edu.iq](mailto:rbadulrahman@uokirkuk.edu.iq)

E-mails addresses: [azhinzainalabbas@uokirkuk.edu.iq](mailto:azhinzainalabbas@uokirkuk.edu.iq), [tamustafa3@uokirkuk.edu.iq](mailto:tamustafa3@uokirkuk.edu.iq)

Received 14/9/2022, Revised 26/11/2022, Accepted 27/11/2022, Published Online First 20/5/2023,  
Published 01/1/2024



This work is licensed under a [Creative Commons Attribution 4.0 International License](https://creativecommons.org/licenses/by/4.0/).

### Abstract:

The fabrication of Solid and Hollow silver nanoparticles (Ag NPs) has been achieved and their characterization was performed using transmission electron microscopy (TEM), zeta potential, UV–VIS spectroscopy, and X-ray diffraction (XRD). A TEM image revealed a quasispherical form for both Solid and Hollow Ag NPs. The measurement of surface charge revealed that although Hollow Ag NPs have a zeta potential of -43 mV, Solid Ag NPs have a zeta potential of -33 mV. According to UV-VIS spectroscopy measurement Solid and Hollow Ag NPs both showed absorption peaks at wavelengths of 436 nm and 412 nm, respectively. XRD pattern demonstrates that the samples' crystal structure is cubic, similar to that of the bulk materials, with average particle sizes of 28 nm and 27 nm for Solid and Hollow Ag NPs, respectively. The antimicrobial activity of synthesized Ag NPs was tested on some pathogenic bacterial strains which were isolated from urinary tract infection (UTI) and burn infection. The experiment results showed positive bactericidal activity against isolated bacteria with Solid Ag NPs which were most effective against both G-ve and G+ve bacteria. In addition, solid nanoparticles showed time and concentration dependent antibacterial activity.

**Keywords:** Ag NPs, Antibacterial, Nanostructure, TEM, Zeta Potential.

### Introduction:

Nanotechnology is the area of research to fabricate and restructure materials on the order of nanometers with a novel properties and functions. There have been ample revolutionary developments in physics, biology, and chemistry that have confirmed the idea of manipulating materials at extremely small scale <sup>1</sup>. The variations in physicochemical characteristics such as light absorption, scattering, electrical and thermal conductivity, melting point, and mechanical properties, which result in enhanced performance over their bulk counterparts, are the factors that lead to a greater contribution in fields of research with a great distinction in technology <sup>2</sup>. The outstanding features of nanoparticles are due to the larger surface area to volume <sup>3,4</sup>. Michael Faraday synthesize a ruby-colored colloidal gold fluid in 1857 <sup>5</sup>, in which a 50 nm gold solution revealed a wine-red color <sup>6</sup>. The nanoscale size range of

nanoparticles is appropriate for circulating in the bloodstream, penetrating cells, and traversing tissues in biological systems <sup>7</sup>.

Traditional medicine has gained popularity as an alternative health system over time, not only in underdeveloped countries but also in developed ones. This alternative medical system has made major inroads into the health-care sector of wealthier countries, where conventional medicine has a stronghold. The traditional knowledge and understanding involved in medication production by certain people have grown in value as traditional medicine has become more widely used around the world. China was the first to use gold-based medical remedies to treat illness, maybe as early as 2500 BC <sup>8</sup>. Bhasma is an herbo-metallic drug (metals such as gold, silver, zinc, calcium, iron, copper, mercury, etc.) that has been utilized in India since ancient times, where they found that the size

of this medicine is usually between 10-50 nm<sup>9</sup>. Mental illnesses and syphilis were treated with colloidal gold during the Middle Ages in Europe<sup>10</sup>. Additionally, nanoparticles can significantly enhance the delivery of drugs due to their potential to enhance blood-brain barrier permeability<sup>11</sup>. Nanotechnology is now one of the most significant technologies in all fields of research.

Silver nanoparticles (Ag NPs) have been studied for a diverse range of applications due to their unique physical and chemical properties at nanoscale, i.e. electrical and thermal conductivities, chemical stability, catalytic and antibacterial activity<sup>12,13</sup>. Ag NPs can disturb functions of cell membranes such as permeability and respiration. Moreover, the penetrated Ag NPs into the bacteria cell can react with Sulfur containing proteins and phosphorus-containing compounds such as deoxyribonucleic acid (DNA) which cause a disturbance in bacteria cells<sup>14,15</sup>. Pathogenic bacteria are bacteria which are capable of causing disease and inflammation when enters the biological system. The traditional technique to treat bacterial infection in the biological system is to use chemical drug (antibiotics). Excessive use of antibiotics can cause bacteria to become increasingly antibiotic resistant<sup>16</sup>. Thus, developing potential and effective medicines with a nanotechnology became an exciting subject especially, when the previous researches showed that difficult for bacterial cells to become resistant to NPs. Hasan and Al-Niaame utilized the rosemary leaves (*Rosmarinus officinalis*) aqueous extract for the biosynthesis of silver nanoparticles and it was efficient against *Pseudomonas aeruginosa* bacteria isolated from wounds<sup>17</sup>. Shareef et al. used *Carthamus oxyacantha* M. Bieb. aqueous extract to fabricate silver nanoparticles with particle sizes between 50–80 nm. They investigated their antibacterial effectiveness against bacteria that were multi-drug resistant (MDR), extremely antibiotic resistant (XDR), and pan drug-resistant (PAN), the examined microorganisms had notable variances in their sensitivity to Ag NPs<sup>18</sup>. Marinescu, et. al. used two methods of synthesis chemical reduction at room temperature (RT) and the solvothermal procedure at high temperature (HT). The particle size of RT method was 1-20 nm and the particle size of HT method was more than 50 nm. HT sample showed relatively better antimicrobial activity and lower agglomeration tendency than Ag NPs prepared at RT<sup>19</sup>. The aim of this study is to fabricate and characterize two different shapes of silver nanoparticles and to assess their antibacterial activity against selected pathogens by *in vitro* susceptibility tests.

## Materials and Methods:

### Materials and equipment's used to fabricate solid and hollow silver nanoparticles

The following are used in this work: Silver Nitrate (AgNO<sub>3</sub>); sodium citrate (Na<sub>3</sub>C<sub>6</sub>H<sub>5</sub>O<sub>7</sub>); glutathione (C<sub>10</sub>H<sub>17</sub>N<sub>3</sub>O<sub>6</sub>S); Sodium borohydride (NaBH<sub>4</sub>); De Ionized sterile water; Aqua regia (concentrated nitric acid and concentrated hydrochloric acid (HNO<sub>3</sub>+3HCl)); three necks round bottom flask; glass reflux condenser; Sensitive electronic balance; hot plate magnetic stirrer; homemade water chiller; centrifuge; ultrasonic cleaner Fig.1.

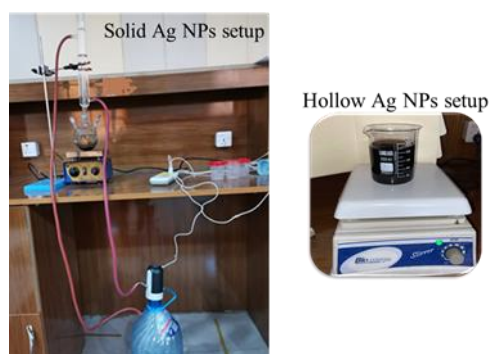
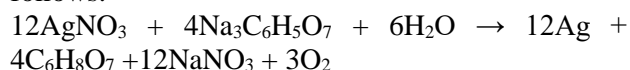


Figure 1. Equipment's used to fabricate Solid and Hollow silver nanoparticles

### Fabrication of solid Ag NPs

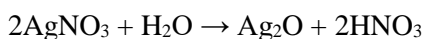
In order to synthesis a solid Ag nanoparticle, silver nitrate (AgNO<sub>3</sub>) was reduced using sodium citrate (Na<sub>3</sub>C<sub>6</sub>H<sub>5</sub>O<sub>7</sub>). Under constant stirring, 250 ml of 0.001M AgNO<sub>3</sub> aqueous solution was heated to boiling. Then 2.5 ml of a 1% Na<sub>3</sub>C<sub>6</sub>H<sub>5</sub>O<sub>7</sub> aqueous solution was added drop-wise. After being heated to a full boil for one hour the colorless solution changed to an olive color, the reaction solution was cooled to room temperature<sup>20</sup>. Using this method, the mechanism of the reaction could be described as follows:



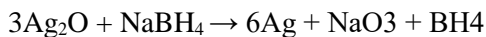
The nanoparticles were centrifuged, cleaned several times with DI water to eliminate any remaining chemicals, and then they were stored for further characterizations.

### Fabrication of Hollow Ag NPs

First, 52 ml of ice-cold water are continuously stirred while aqueous solutions of AgNO<sub>3</sub> (3 ml, 0.01 M), and glutathione (C<sub>10</sub>H<sub>17</sub>N<sub>3</sub>O<sub>6</sub>S) (0.36 ml, 0.01 M) are also added as a capping agent. This produces silver oxide (Ag<sub>2</sub>O) nanoparticles, which are the precursor to Hollow Ag nanoparticles. The mechanism of the reaction could be described as follows:



Then, 3.6 ml of freshly prepared 0.01 M Sodium borohydride ( $\text{NaBH}_4$ ) solution was added all at once to the generated pale yellowish solution of  $\text{Ag}_2\text{O}$  nanoparticles. The reaction mixture turns orange as Hollow Ag nanostructures are formed from  $\text{Ag}_2\text{O}$  nanoparticles<sup>21</sup>. The mechanism of the reaction could be described as follows:



The nanoparticles were centrifuged, cleaned several times with DI water to eliminate any remaining chemicals, and then they were stored for further characterizations.

### Characterization of silver nanoparticles

A double beam ultraviolet-visible (UV-Vis) spectrophotometer (T92+ UV Spectrophotometer, PG INSTRUMENTS) was used to measure the formation of Ag NPs in order to assess the effectiveness of the chemical reduction of silver nitrate. A cuvette with a 1 cm distance was filled with materials for analysis. Readings from 350 to 750 nm were scanned at intervals of 2 nm for the UV-Vis spectrophotometric measurements. Using a ZEISS (EM10C) Transmission Electron Microscope (TEM) (100Kv), the morphologies of the synthesized Ag NPs were examined. With the use of the DX-2700BH Multipurpose X-ray Diffractometer, patterns of the produced Ag NPs were acquired using X-ray Diffraction (XRD). The Zeta Potential of Ag NPs measured by HORIBA SZ-100 to determine the stability and surface charge of the particles. The EC/TDS and temperature meters HI 99300 device was used to determine the concentration of Solid and Hollow Ag NPs.

### Concentration of synthesized Ag NPs

A serial of concentrations was prepared for Solid and Hollow silver nanoparticles. Then, the standard solution was diluted with deionized water by following Eq.1:

$$C_1 V_1 = C_2 V_2 \quad 1$$

$C_1$  stock solution concentration,  $V_1$  stock solution volume,  $C_2$  final solution concentration, and  $V_2$  final solution volume.

The concentrations which calculated by Eq. 1 are as the following (380, 300, 200, 100, 50, 10)  $\mu\text{g/mL}$  for Solid Ag NPs and (2000, 300, 200, 100, 50, 10)  $\mu\text{g/mL}$  for Hollow Ag NPs.

### Sample collection

Bacterial samples were collected from patients with urinary tract infection (UTI) and burn infections in Kirkuk and Azadi Hospital / Kirkuk Governorate from 1/12/2021 to 1/5 of 2022. The samples were examined under light microscope and

differentiated by using Gram stain then stored in nutrient agar media.

### Maintenance of bacterial samples

The isolated samples were maintained on nutrient agar culture. The medium was prepared as recommended by manufactured company by dissolving 28g of nutrient agar in 1000 ml of distilled water, pH was adjusted to 7-7.2. and sterilized using autoclave at  $121^\circ\text{C}$ ,  $1.25\text{kg/cm}^2$  for 15 min. Bacterial strains were activated 24 hours before use and incubated at  $37^\circ\text{C}$ . For long time maintenance, 85 ml of Nutrient broth was prepared and 15 ml of glycerol were added to the medium. The samples were grown and incubated at a of  $37^\circ\text{C}$  for 24 hours, and then kept in the freezer at  $-20^\circ\text{C}$  until use.

### Preparation of bacterial suspension for sensitivity test

A sufficient quantity of pure bacterial colonies was transferred by a sterile loop to a test tube containing 5 ml of sodium chloride sterile normal saline to suspend cells. The bacterial suspension was compared with 0.5 standard fixed McFarland's solution to give an approximate number for bacterial growth of  $1.5 \times 10^8$  cells/ml<sup>22</sup>.

### Antimicrobial activity of Ag NPs (sensitivity test):

#### Disk diffusion methods (Kirby-Bauer disk)

The antibacterial activity of chemically synthesized Ag NPs was analyzed by agar-disk diffusion method against both Gram-positive and Gram-negative bacterial strains. The bacterial suspension was incubated for 24-48 hours to test. Isolated bacteria were inoculated on the sterilized Muller-Hinton agar plate and allowed to dry for 5 min. A sterilized disk was loaded with specific concentration of Solid or Hollow Ag NPs. The disk was pressed down tightly to make contact with the surface of the plate. The inoculated plate was incubated at  $37^\circ\text{C}$  for 24 hours. Later, the inhibition zone around each disk was measured by ruler expressed by millimeter (mm) and recorded.

#### Agar well diffusion method

Antimicrobial activity of Solid and Hollow Ag NPs was also evaluated by agar well diffusion method. The activated bacteria were inoculated on sterilized Muller-Hinton agar plates and allowed to dry for 5 min. Then a hole with a diameter of 6 mm is punched using sterilized tip and a volume of  $100\mu\text{l}$  at desired concentration from Solid and Hollow Ag NPs introduced into the well. The plate was inoculated at  $37^\circ\text{C}$  for 24 hours. Later, the

inhibition zone around each hole was measured and recorded.

## Results and Discussion:

### Visual observation of nanoparticles formations

The visual observation of the solution's color changing from colorless to olive for Solid Ag NPs

and orange for Hollow Ag NPs upon heating provided as visual confirmation of the production of silver nanoparticles (the reduction process of  $\text{Ag}^+$  to  $\text{Ag}^0$  nanoparticles) as shown in Fig. 2.



Solid Ag NPs

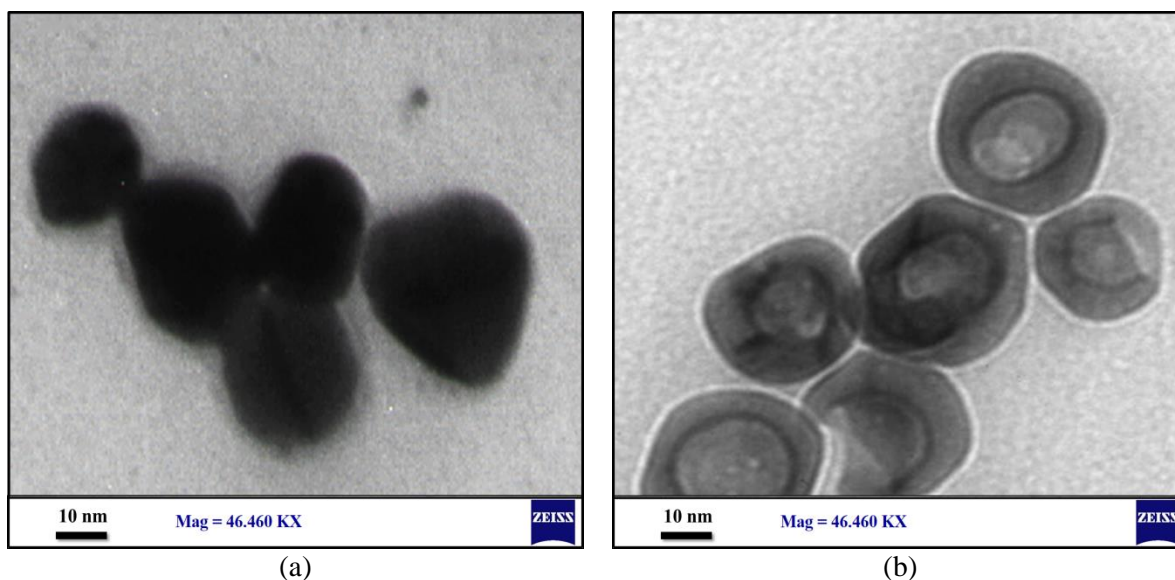
Hollow Ag NPs

Figure 2. Visual identification of nanoparticles formation.

### TEM analysis

The interaction between a high-energy electron beam and a solid material is the basis for Transmission Electron Microscope (TEM) images. Fig.3 shows a TEM image for analyzing the particle size and shape of the solid and Hollow Ag NPs.

From Fig.3a quasispherical shape can be observed with average size of  $\sim 30$  nm for solid Ag NPs, while for Hollow Ag NPs the outer diameter is  $\sim 30$  nm and the inner diameter is  $\sim 20$  nm as can be seen in Fig.3b which is comparable to Abdulrahman's<sup>21</sup> results..



(a)

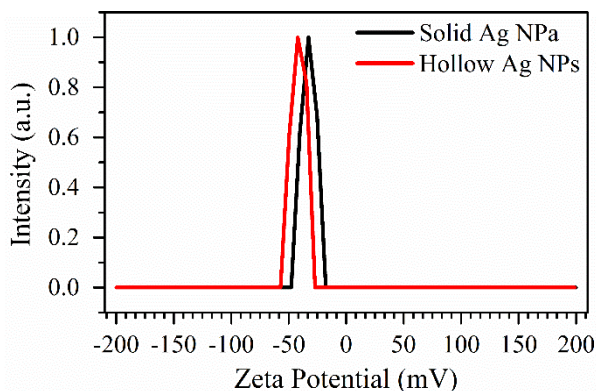
(b)

Figure 3. TEM image of (a) Solid and (b) Hollow Ag NPs.

### Zeta potential analysis

The effective electric charge on the surface of a nanoparticle is measured by its zeta potential. The zeta potential's magnitude gives information on the stability of the particles<sup>23</sup>. Values between 30 and 40 mV (positive or negative) exhibit moderate stability; however, values between 40 and 60 mV may be indications of strong stability<sup>24</sup>. Low zeta potential nanoparticles will eventually aggregate

due to Vander Waal inter-particle interactions<sup>25</sup>. Therefore, Hollow Ag NPs have a Zeta Potential value of  $-43$  mV, indicating high stability, compared to solid Ag NPs, which have a Zeta Potential value of  $-33$  mV Fig. 4. The Zeta Potential value is influenced by fabrication techniques and nanoparticles environment<sup>26</sup>.



**Figure 4. Zeta Potential of Solid and Hollow Ag NPs.**

### UV-Vis spectra analysis

One of the most commonly used methods for characterizing the optical properties of silver nanoparticles is UV-Visible spectroscopy. Considering that silver nanoparticles have a high absorption peak as a result of surface plasmon excitation, it is quite sensitive to the presence of silver colloids<sup>27</sup>. The absorption spectra of the solid and hollow silver nanoparticles are shown in Fig. 5. The plasmon resonance absorption peak of the solid and hollow nanoparticles is observed at wavelength 436 nm and 412 nm, respectively. The surface plasmon resonance (SPR) absorption peak is developed by the simultaneous vibration of the free electrons in metal nanoparticles (NPs) in resonance with the light wave, and in contrast to semiconductor or insulator nanomaterials, the optical properties of metal nanostructures are more sensitive to shape and less responsive to size<sup>27</sup>. For solid metal NPs, the absorption peak shifts to the

red because the particle becomes more oblate according to the previous study<sup>28</sup>, as observed in TEM images Fig. 3.

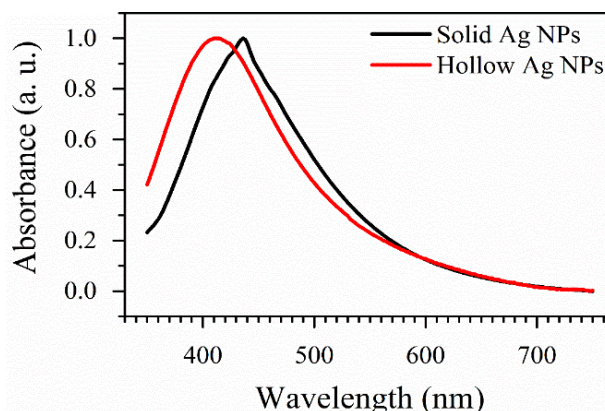


**Figure 5. Absorbance spectrum of Solid and Hollow Ag NPs.**

According to Tauc's plot, which is depicted in Fig. 6, the direct band gap of silver nanoparticles was estimated to be 2.28 eV for Solid Ag NPs and 2.34 eV for Hollow Ag NPs. This result is quite similar to the previously reported band gap for silver nanoparticles, which is approximately 2.20 eV<sup>29</sup>. The synthesis method influences the band gap of silver nanoparticles since the band gap increases as the particle size reduces. As the grain size increases, the particles' optical band gap reduces. The rise in the barrier height at the grain boundary brought on by an increase in grain size causes the band gap of the particles to reduce<sup>30</sup>.

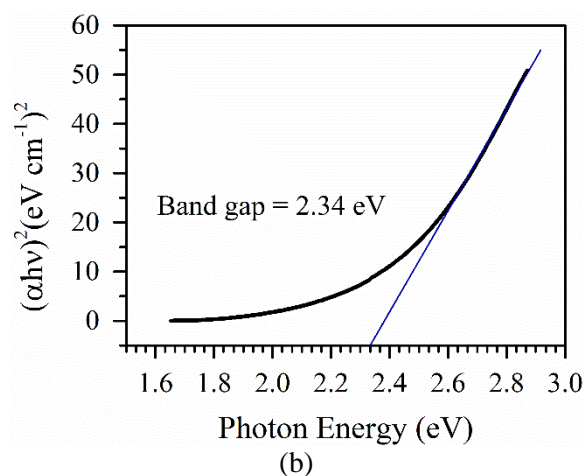
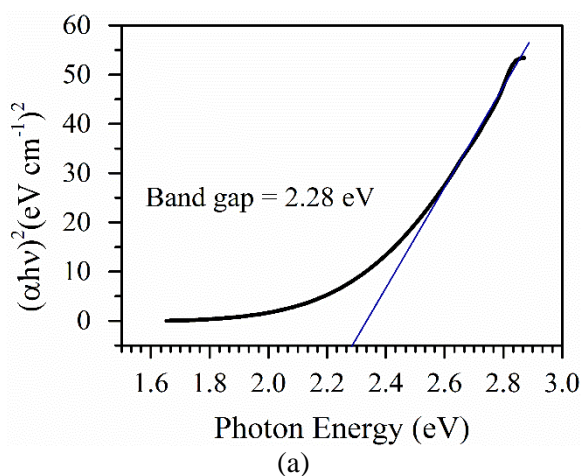


**Figure 6. Calculated Band gap of (a) Solid and (b) Hollow Ag NPs.**

### XRD analysis

The crystal planes of thin films and nanostructures that are parallel to the substrate surface can be identified using the XRD technique.

Fig. 7 displays the XRD results for Solid and Hollow Ag NPs. Both samples exhibit polycrystalline structure with (111), (200), (220), and (311) orientations appearing at diffraction

angles of 38.1, 44.2, 64.4, and 77.4, respectively (ICDD no: 00-004-0783) it can be assigned to the cubic structure. The samples are single-phase, according to the XRD pattern, and only the distinctive diffraction peaks of the FCC phase of Ag were seen with a lattice constant  $a \sim 4.08\text{\AA}$  which agrees with the previously reported results<sup>31</sup>. With the use of the Scherrer Equation<sup>32</sup> (Eq. 2),

$$D = 0.9\lambda / \beta \cos\theta \quad 2$$

D is the crystallite size,  $\theta$  is the Bragg angle,  $\lambda$  is the X-ray wavelength, and  $\beta$  is full width at half maximum (FWHM).

According to Eq. 2 the average crystallite size for Solid and Hollow Ag NPs, respectively, was determined to be about 22 nm and 25 nm, which is quite consistent with the average particle diameter observed in Fig. 3's TEM images, which is close to the nanoparticles fabricated previously<sup>21</sup>. Table 1 lists the fitting results for all samples.

**Table 1. Lattice parameter of Solid and Hollow Ag NPs.**

samples	(hkl)	FWHM (Å)	$d_{hkl}$ (Å)	D (nm)
Solid Ag NPs	(111)	0.14767	2.3557	28.19646
	(200)	0.14929	2.04	24.05144
	(220)	0.10221	1.4427	24.1345
	(311)	0.15622	1.2302	13.15566
Hollow Ag NPs	(111)	0.15151	2.3557	27.48182
	(200)	0.10486	2.04	34.24222
	(220)	0.14158	1.4427	17.42328
	(311)	0.08434	1.2302	24.36777

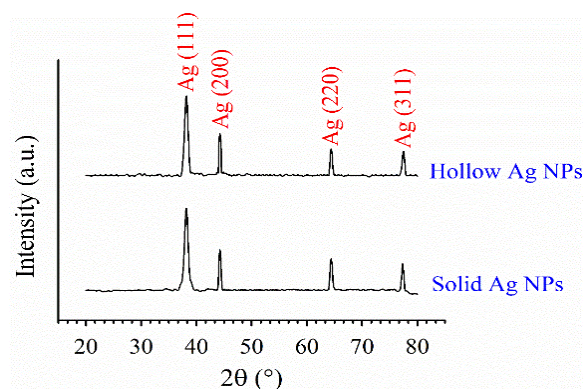


**Figure 7. XRD pattern of Solid and Hollow Ag NPs.**

### Antibacterial activity analysis

The sensitivity test was conducted to evaluate the antibacterial activity of synthesized Ag NPs. Disk and well diffusion in vitro antimicrobial screening methods are the basic, well known and most applied procedures in microbiology lab. The antimicrobial activity of both Solid and Hollow Ag NPs was tested by applying serial of nanoparticles concentration. Generally, Solid Ag NPs showed efficient antibacterial activity than Hollow Ag NPs with most concentrations used in this study and were active against both G<sup>-ve</sup> and G<sup>+ve</sup> bacterial strains. In addition to, the Solid Ag NPs showed clear inhibition zone in both sensitivity tests used in experimental part.

The well respond bacterial strain to solid nanoparticles in well diffusion agar method are *E.coli*, from burn infection as well as *S. aureus*, *Klebsiella*, and *Proteus* from UTI infection which gave a clear inhibition zone of 12 mm in Fig. 8 (*E. coli* No.6, *S. aureus* No.10, *Klebsiella* No.11, *Proteus* No.12) after 24 hours when exposed to highest concentration 380  $\mu\text{g/ml}$  Ag NPs Fig. 9a. The nanotoxicity of Solid Ag NPs showed a direct relationship with concentration, the antibacterial activity increased as the concentration of nanoparticles increased. When low concentrations (50 and 10  $\mu\text{g/ml}$ ) applied, no inhibition zone appeared with most bacterial isolates except for *E.coli* No. 6 in Fig. 9a which isolated from burn infection showed an inhibition zone of 6 mm appeared after 24 hours of incubation. On the other hands, *Klebsiella* No. 11 in Fig. 9b which isolated from UTI infection also responded to low concentrations of nanoparticles after 48 hours of incubation.

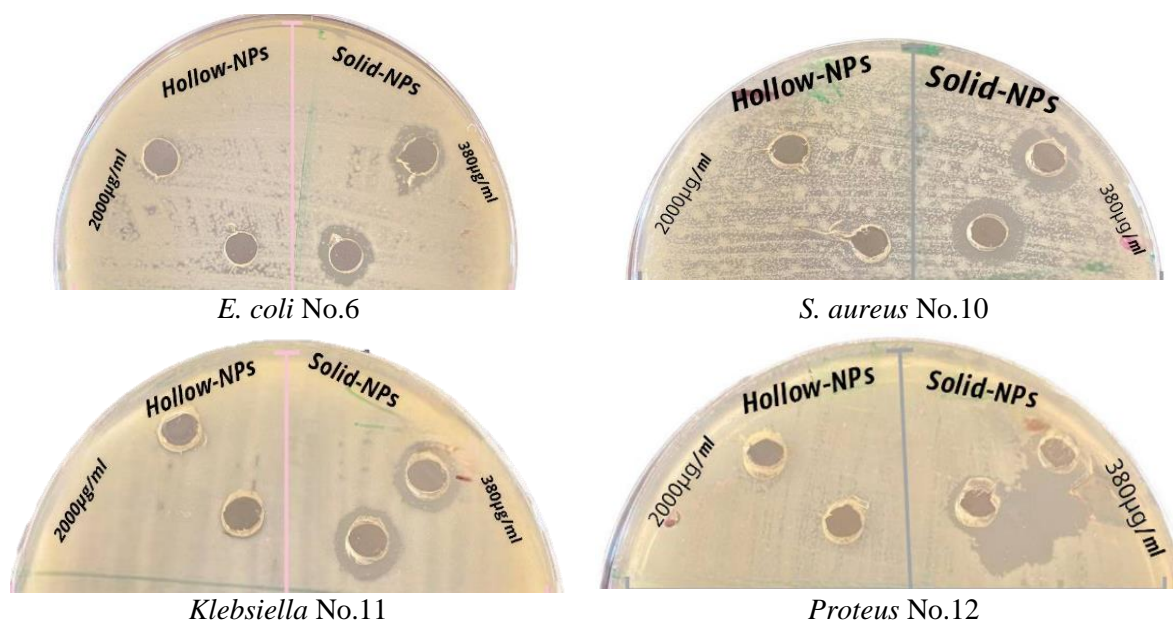


Figure 8. The inhibition zone by agar well diffusion method. bacteria exposed to 380µg/ml of solid Ag NPs for 24 hours

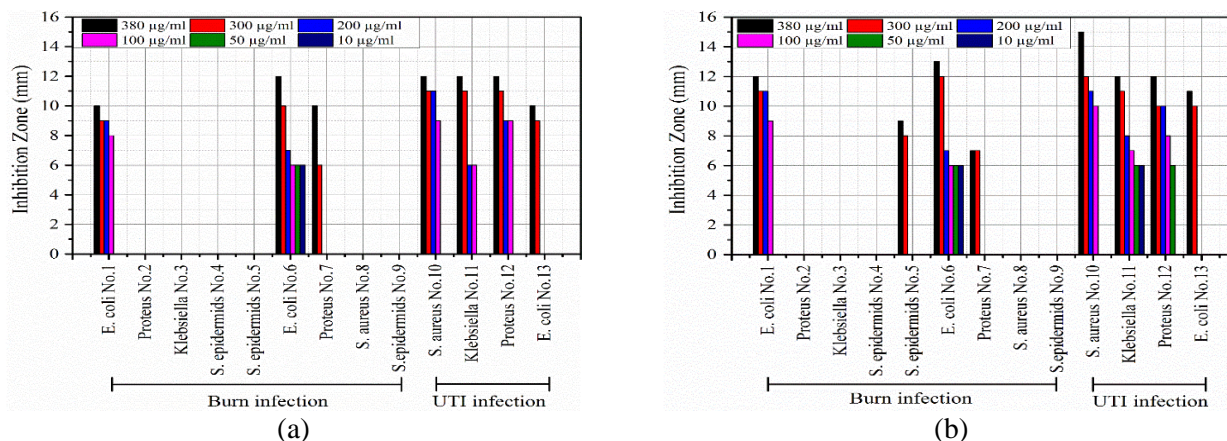


Figure 9. Zone of inhibition for Solid Ag NPs after (a) 24 hours and (b) 48 hours by agar well diffusion method.

Similar results were proved with disk diffusion method Fig. 10 *E. coli* No.1 from burn infection well responded to high concentrations of AgNPs (380 and 300 µg/ml) which showed the largest inhibition zone of 19 and 16 mm respectively after 24 hours of incubation Fig. 11a while the zone diameter increased which became 22 and 20 mm after 48 hours Fig. 11b for both concentrations. *E. coli* from UTI infection also

showed positive response to high concentration of solid AgNPs. Nevertheless, G-ve bacterial strains were more sensitive to solid Ag NPs than G+ve bacterial strains. The inhibition zone of Solid Ag NPs for all samples was tabulated in Table 2 (agar well diffusion method) and Table 3 (agar disc diffusion method) which is in a good agreement with previous studies<sup>13</sup>.

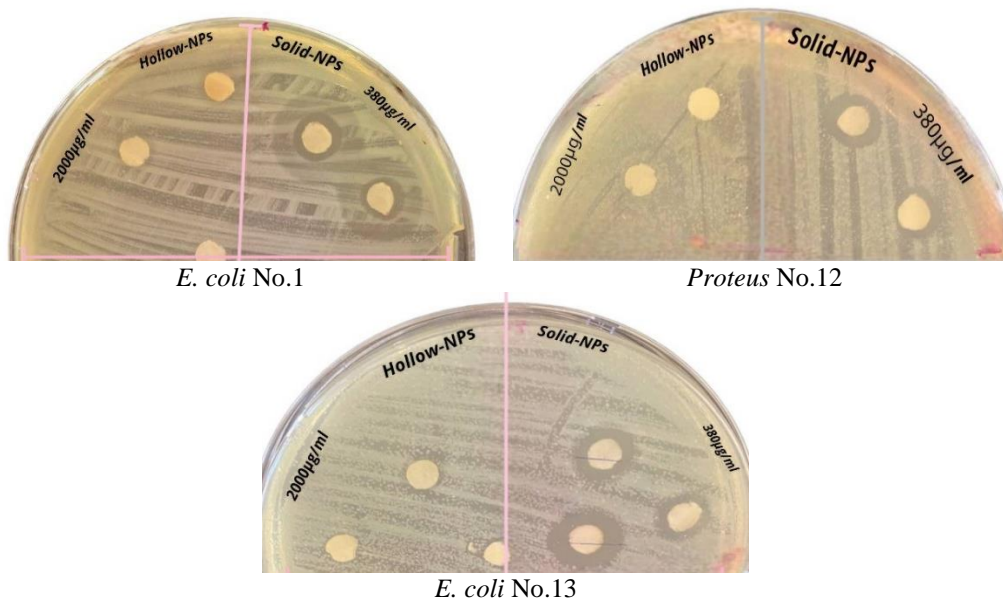


Figure 10. The inhibition zone by agar disc diffusion method. bacteria exposed to 380µg/ml of solid Ag NPs for 24 hours

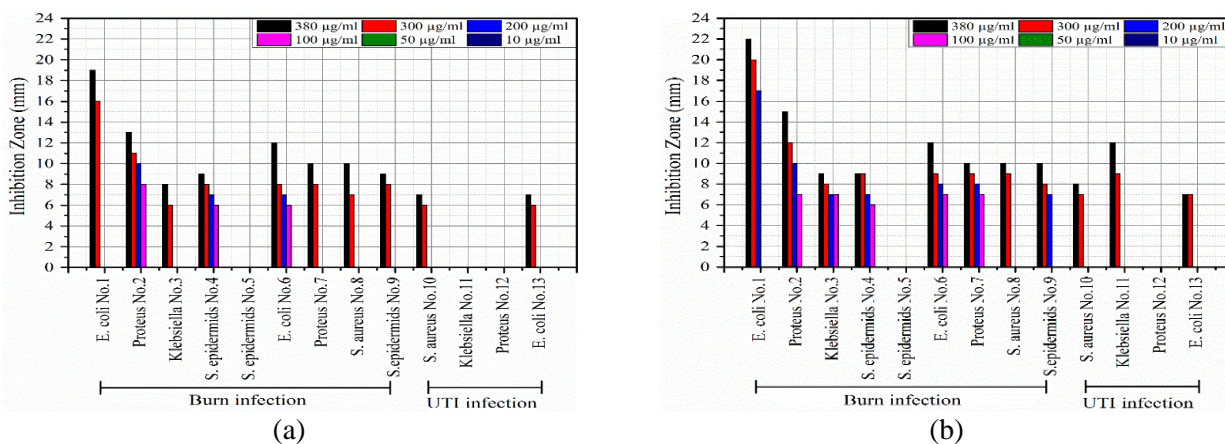


Figure 11. Zone of inhibition for Solid Ag NPs after (a) 24 hours and (b) 48 hours by agar disc diffusion method

Table 2. Zone of inhibition for Solid Ag NPs by agar well diffusion method.

No.	Bacteria Isolates	Gram stain	Inhibition zone (mm) After 24 hours						Inhibition zone (mm) After 48 hours					
			380 µg/ml	300 µg/ml	200 µg/ml	100 µg/ml	50 µg/ml	10 µg/ml	380 µg/ml	300 µg/ml	200 µg/ml	100 µg/ml	50 µg/ml	10 µg/ml
<b>Burn</b>														
1	<i>E. coli</i>	-	10	9	9	8	0	0	12	11	11	9	0	0
2	<i>Proteus</i>	-	0	0	0	0	0	0	0	0	0	0	0	0
3	<i>Klebsiella</i>	-	0	0	0	0	0	0	0	0	0	0	0	0
4	<i>S. epidermids</i>	+	0	0	0	0	0	0	0	0	0	0	0	0
5	<i>S. epidermids</i>	+	0	0	0	0	0	0	9	8	0	0	0	0
6	<i>E. coli</i>	-	12	10	7	6	6	6	13	12	7	6	6	6
7	<i>Proteus</i>	-	10	6	0	0	0	0	7	7	0	0	0	0
8	<i>S. aureus</i>	+	0	0	0	0	0	0	0	0	0	0	0	0
9	<i>S. epidermids</i>	+	0	0	0	0	0	0	0	0	0	0	0	0
<b>Urinary Tract Infection (UTI)</b>														
10	<i>S. aureus</i>	+	12	11	11	9	0	0	15	12	11	10	0	0
11	<i>Klebsiella</i>	-	12	11	6	6	0	0	12	11	8	7	6	6
12	<i>Proteus</i>	-	12	11	9	9	0	0	12	10	10	8	6	0
13	<i>E. coli</i>	-	10	9	0	0	0	0	11	10	0	0	0	0

**Table 3. Zone of inhibition for Solid Ag NPs by agar disc diffusion method.**

No.	Bacteria Isolates	Gram stain	Inhibition zone (mm) After 24 hours						Inhibition zone (mm) After 48 hours					
			380	300	200	100	50	10	380	300	200	100	50	10
			$\mu\text{g/ml}$	$\mu\text{g/ml}$	$\mu\text{g/ml}$	$\mu\text{g/ml}$	$\mu\text{g/ml}$	$\mu\text{g/ml}$	$\mu\text{g/ml}$	$\mu\text{g/ml}$	$\mu\text{g/ml}$	$\mu\text{g/ml}$	$\mu\text{g/ml}$	$\mu\text{g/ml}$
<b>Burn</b>														
1	<i>E. coli</i>	-	19	16	0	0	0	0	22	20	17	0	0	0
2	<i>proteus</i>	-	10	8	0	0	0	0	10	9	8	7	0	0
3	<i>Klebsiella</i>	-	0	0	0	0	0	0	0	0	0	0	0	0
4	<i>S. epidermids</i>	+	0	0	0	0	0	0	12	9	0	0	0	0
5	<i>S. epidermids</i>	+	0	0	0	0	0	0	0	0	0	0	0	0
6	<i>E. coli</i>	-	8	6	0	0	0	0	9	8	7	7	0	0
7	<i>proteus</i>	-	10	7	0	0	0	0	10	9	0	0	0	0
8	<i>S. aureus</i>	+	7	6	0	0	0	0	8	7	0	0	0	0
9	<i>S. epidermids</i>	+	7	6	0	0	0	0	7	7	0	0	0	0
<b>Urinary Tract Infection (UTI)</b>														
10	<i>S. aureus</i>	+	9	8	0	0	0	0	10	8	7	0	0	0
11	<i>Klebsiella</i>	-	9	8	7	6	0	0	9	9	7	6	0	0
12	<i>Proteus</i>	-	12	8	7	6	0	0	12	9	8	7	0	0
13	<i>E. coli</i>	-	13	11	10	8	0	0	15	12	10	7	0	0

Hollow Ag NPs showed no antibacterial activity against all bacterial strains and all concentrations used in both tests Table 4 and Table 5. Hollow silver nanoparticles appeared to have no bactericidal effect on the tested bacterial strain because bacterial cell surfaces have a negative electrostatic charge<sup>33</sup> and Hollow Ag NPs have a larger negative surface charge (-43 mV), which will repel<sup>34</sup> bacteria cells with a greater electrostatic force (Coulomb force) than Solid Ag NPs. Previous studies proved that surface of Ag NPs plays a critical role in their antimicrobial activity, positively charged exhibit the highest antibacterial activity<sup>35</sup>. Ag NPs are preferred in medical applications because their small size that helps to reach vital areas within the living microorganism add to it, Ag NPs exert more efficient antimicrobial activity rather than silver salt<sup>36</sup>. In addition, silver ions have high toxic effect against microbes rather than mammalian cells<sup>37</sup>.

Ag NPs' mechanism of action against bacteria is still not well understood. However, a number of theories are offered to account for silver nanoparticle's antibacterial properties: (1) Nanoparticles are known to have an enormous surface area which either penetrates the bacteria cell

or connects to the cell wall, disrupting the membrane's permeability and makes it porous, which causes further leaking of cell content<sup>38</sup>. Additionally, the development of membrane pores causes the flow of nanoparticles into the cell, where they connect with proteins that contain sulfur and phosphorus, inactivating proteins and DNA<sup>39</sup>. (2) Since Ag<sup>+</sup> ions are released during the oxidation reduction process, Ag NPs have an antimicrobial effect. The primary interactions between the oxidized silver ions from Ag NP and the thiol groups of several enzymes and proteins are what breakdown the bacterial cell wall and interfere with the respiratory chain<sup>39</sup>. (3) Reactive oxygen species (ROS), which are regarded to be the main cause of the majority of bacterial cell deaths, are made impossible to produce by silver ions due to the suppression of ATP production and DNA replication<sup>18,39</sup>. Previous report proved the action of Ag NPs on the morphology of *S. aureus* and *C. albicans*, incubation of bacteria with Ag NPs for 12 hours lead to cell lysis, breakdown of bacterial cell wall compares to control sample as revealed by transmission electron microscope (TEM) these series of events lead to cell death after releasing inside components to surrounding environment<sup>14</sup>.

**Table 4. Zone of inhibition for Hollow Ag NPs by agar well diffusion method.**

No.	Bacteria Isolates	Gram stain	Inhibition zone (mm) After 24 hours						Inhibition zone (mm) After 48 hours					
			2000 µg/ml	300 µg/ml	200 µg/ml	100 µg/ml	50 µg/ml	10 µg/ml	2000 µg/ml	300 µg/ml	200 µg/ml	100 µg/ml	50 µg/ml	10 µg/ml
<b>Burn</b>														
1	<i>E. coli</i>	-	0	0	0	0	0	0	0	0	0	0	0	0
2	<i>Proteus</i>	-	0	0	0	0	0	0	0	0	0	0	0	0
3	<i>Klebsiella</i>	-	0	0	0	0	0	0	0	0	0	0	0	0
4	<i>S. epidermids</i>	+	0	0	0	0	0	0	0	0	0	0	0	0
5	<i>S. epidermids</i>	+	0	0	0	0	0	0	0	0	0	0	0	0
6	<i>E. coli</i>	-	0	0	0	0	0	0	0	0	0	0	0	0
7	<i>Proteus</i>	-	0	0	0	0	0	0	0	0	0	0	0	0
8	<i>S. aureus</i>	+	0	0	0	0	0	0	0	0	0	0	0	0
9	<i>S. epidermids</i>	+	0	0	0	0	0	0	0	0	0	0	0	0
<b>Urinary Tract Infection (UTI)</b>														
10	<i>S. aureus</i>	+	0	0	0	0	0	0	0	0	0	0	0	0
11	<i>Klebsiella</i>	-	0	0	0	0	0	0	0	0	0	0	0	0
12	<i>Proteus</i>	-	0	0	0	0	0	0	0	0	0	0	0	0
13	<i>E. coli</i>	-	0	0	0	0	0	0	0	0	0	0	0	0

**Table 5. Zone of inhibition for Hollow Ag NPs by agar disc diffusion method.**

No.	Bacteria Isolates	Gram stain	Inhibition zone (mm) After 24 hour						Inhibition zone (mm) After 48 hours					
			2000 µg/ml	300 µg/ml	200 µg/ml	100 µg/ml	50 µg/ml	10 µg/ml	2000 µg/ml	300 µg/ml	200 µg/ml	100 µg/ml	50 µg/ml	10 µg/ml
<b>Burn</b>														
1	<i>E. coli</i>	-	0	0	0	0	0	0	0	0	0	0	0	0
2	<i>Proteus</i>	-	0	0	0	0	0	0	0	0	0	0	0	0
3	<i>Klebsiella</i>	-	0	0	0	0	0	0	0	0	0	0	0	0
4	<i>S. epidermids</i>	+	0	0	0	0	0	0	0	0	0	0	0	0
5	<i>S. epidermids</i>	+	0	0	0	0	0	0	0	0	0	0	0	0
6	<i>E. coli</i>	-	0	0	0	0	0	0	0	0	0	0	0	0
7	<i>Proteus</i>	-	0	0	0	0	0	0	0	0	0	0	0	0
8	<i>S. aureus</i>	+	0	0	0	0	0	0	0	0	0	0	0	0
9	<i>S. epidermids</i>	+	0	0	0	0	0	0	0	0	0	0	0	0
<b>Urinary Tract Infection (UTI)</b>														
10	<i>S. aureus</i>	+	0	0	0	0	0	0	0	0	0	0	0	0
11	<i>Klebsiella</i>	-	0	0	0	0	0	0	0	0	0	0	0	0
12	<i>Proteus</i>	-	0	0	0	0	0	0	0	0	0	0	0	0
13	<i>E. coli</i>	-	0	0	0	0	0	0	0	0	0	0	0	0

**Conclusion:**

Transmission electron microscopy (TEM), Zeta potential, UV-VIS spectroscopy, and X-ray diffraction were used to characterize the Solid and Hollow silver nanoparticles (Ag NPs) that were synthesized by chemical reduction of Silver Nitrate. Both Hollow and Solid Ag NPs have a quasispherical shape, according to a TEM image. Although Hollow Ag NPs have a zeta potential of -43 mV, Solid Ag NPs have a zeta potential of -33 mV, according to the Zeta potential measurement. UV-VIS spectroscopy measurements revealed that both Solid and Hollow Ag NPs showed a sharp peak at wavelengths of 436 nm and 412 nm, respectively. According to XRD results, the samples' cubic crystal structure is identical to that of

the bulk materials, and their typical particle sizes, as determined by Scherrer equation for Solid and Hollow Ag NPs, respectively, are approximately 28 nm and 27 nm. The Solid Ag NPs showed clear inhibition zone in sensitivity tests which proves their antibacterial activity revealed broad spectrum antimicrobial activity against G-ve and G+ve bacteria compared to Hollow particles. In addition to, the antimicrobial activity of synthesized silver nanoparticles was stimulated in time and concentration- dependent manner. We showed, based on the findings of this study, that the surface charge of nanoparticles is crucial for antimicrobial sensitivity tests.

**Acknowledgment:**

The authors gratefully acknowledge the Department of Chemistry, the Department of Biology, and Environmental Researches Unit College of Science University of Kirkuk Iraq for their assistance.

**Authors' Declaration:**

- Conflicts of Interest: None.
- We hereby confirm that all the Figures and Tables in the manuscript are mine ours. Besides, the Figures and images, which are not mine ours, have been given the permission for re-publication attached with the manuscript.
- Authors sign on ethical consideration's approval
- Ethical Clearance: The project was approved by the local ethical committee in University of Kirkuk.

**Authors' Contributions Statement:**

The proposed idea was conceived by R. B. A. The data was acquired by A. Z. A. The analysis was carried out by A. Z. A, R. B. A, and T. A. M. The data were interpreted by R. B. A and T. A. M. The paper's drafter is A. Z. A. The article was revised and proofread by R. B. A and T. A. M. All authors read the manuscript carefully and approve the final version of their MS.

**References:**

1. Abdullah MF, Abdulrahman RB. The Electrical and Optical properties of Copper Oxide Nanostructures fabricated by Hot Deionized Water Copper Treatment. *Eurasian J Phys Chem Math.* 2022 August; 9(SE): 45–53.
2. Chuang ST, Conklin B, Stein JB, Pan G, Lee K-B. Nanotechnology-enabled immunoengineering approaches to advance therapeutic applications. *Nano Conver.* 2022 April; 9(1): 1-31. <https://doi.org/10.1186/s40580-022-00310-0>.
3. Sadovnikov SI, Gusev AI. Effect of Particle Size and Specific Surface Area on the Determination of the Density of Nanocrystalline Silver Sulfide Ag<sub>2</sub>S Powders. *Phys Solid State.* 2018 May; 60(5): 877–881. <https://doi.org/10.1134/S106378341805027X>.
4. Zhang J, Li Y, Cao K, Chen R. Advances in Atomic Layer Deposition. *Nanomanuf Metrol.* 2022 September; 5(3): 191–208. <https://doi.org/10.1007/s41871-022-00136-8>.
5. Faraday M. LIX Experimental relations of gold (and other metals) to light- The bakerian lecture. London, Edinburgh, Dublin Philos Mag J Sci. 1857 January; 14(96): 512–539. <https://doi.org/10.1080/14786445708642424>
6. Dong YC, Hajfathalian M, Maidment PSN, Hsu JC, Naha PC, Si-Mohamed S, et al. Effect of Gold Nanoparticle Size on Their Properties as Contrast Agents for Computed Tomography. *Sci Rep.* 2019 December; 9(1): 14912. <https://doi.org/10.1038/s41598-019-50332-8>.
7. Ye H, Shen Z, Yu L, Wei M, Li Y. Manipulating nanoparticle transport within blood flow through external forces: an exemplar of mechanics in nanomedicine. *Proc R Soc A Math Phys Eng Sci.* 2018 March; 474(2211): 20170845. <https://doi.org/10.1098/rspa.2017.0845>
8. Major JS. Science and Civilisation in China. Vol. 5: Chemistry and Chemical Technology; Pt. 2: Spagyric Discovery and Invention: Magisteries of Gold and Immortality. *Technol Cult.* 1975 October; 16(4): 621–627. <https://doi.org/10.2307/3103442>.
9. Pathiraja PMYS, Ranatunga YMMK, Herapathdeniya SKMK, Gunawardena SHP. Swarna Makshika Bhasma preparation using an alternative heating method to traditional Varaha Puta. *J Ayurveda Integr Med.* 2020 July; 11(3): 206–212. <https://doi.org/10.1016/j.jaim.2018.02.136>
10. Dykman L, Khlebtsov N. Gold nanoparticles in biomedical applications: recent advances and perspectives. *Chem Soc Rev.* 2012 May; 41(6): 2256–2282. <https://doi.org/10.1039/C1CS15166E>.
11. Zorkina Y, Abramova O, Ushakova V, Morozova A, Zubkov E, Valikhov M, et al. Nano Carrier Drug Delivery Systems for the Treatment of Neuropsychiatric Disorders: Advantages and Limitations. *Molecules.* 2020 November; 25(22): 5294. <https://doi.org/10.3390/molecules25225294>.
12. Khan I, Saeed K, Khan I. Nanoparticles: Properties, applications and toxicities. *Arab J Chem.* 2019 November; 12(7): 908–931. <https://doi.org/10.1016/j.arabjc.2017.05.011>.
13. Shareef HA, Jafar NB, Abdulrahman RB. The Biosynthesis of Silver Nanoparticles by Moringa Oleifera and its Antibacterial Activity. *Indian J Public Heal Res Dev.* 2019 August; 10(8): 2052.
14. Dorgham RA, Abd Al Moaty MN, Chong KP, Elwakil BH. Molasses-Silver Nanoparticles: Synthesis, Optimization, Characterization, and Antibiofilm Activity. *Int J Mol Sci.* 2022 September; 23(18): 10243. <https://doi.org/10.3390/ijms231810243>
15. Sampath G, Chen Y-Y, Rameshkumar N, Krishnan M, Nagarajan K, Shyu DJH. Biologically Synthesized Silver Nanoparticles and Their Diverse Applications. *Nanomaterials.* 2022 September; 12(18): 3126. <https://doi.org/10.3390/nano12183126>.
16. Xavier SP, Victor A, Cumaquela G, Vasco MD, Rodrigues OAS. Inappropriate use of antibiotics and its predictors in pediatric patients admitted at the Central Hospital of Nampula, Mozambique. *Antimicrob Resist Infect Control.* 2022 December; 11(1): 79. <https://doi.org/10.1186/s13756-022-01115-w>
17. Sura S, Hasan, Asmaa E. Al-Niaame. Study of Biosynthesis, Characterization and Antibacterial Activity of Silver Nanoparticles against Pseudomonas Aeruginosa Isolated From Wounds from Some Baghdad Hospitals. *J Coll basic Educ.* 2022 March; 26(107): 1–16.
18. Shareef AA, Hassan ZA, Kadhim MA, Al-Mussawi

- AA. Antibacterial Activity of Silver Nanoparticles Synthesized by Aqueous Extract of *Carthamus oxyantha* M.Bieb. Against Antibiotics Resistant Bacteria. *Baghdad Sci J*. 2022 June; 19(3): 460–468. <https://doi.org/10.21123/bsj.2022.19.3.0460>
19. Marinescu L, Fikai D, Fikai A, Oprea O, Nicoara AI, Vasile BS, et al. Comparative Antimicrobial Activity of Silver Nanoparticles Obtained by Wet Chemical Reduction and Solvothermal Methods. *Int J Mol Sci*. 2022 May; 23(11): 5982. <https://doi.org/10.3390/ijms23115982>
20. Abdulrahman HB, Krajczewski J, Kudelski A. Modification of surfaces of silver nanoparticles for controlled deposition of silicon, manganese, and titanium dioxides. *Appl Surf Sci*. 2018 January; 427: 334–339. <https://doi.org/10.1016/j.apsusc.2017.08.163>
21. Abdulrahman HB, Kołataj K, Lenczewski P, Krajczewski J, Kudelski A. MnO<sub>2</sub>-protected silver nanoparticles: New electromagnetic nanoresonators for Raman analysis of surfaces in basis environment. *Appl Surf Sci*. 2016 December; 388: 704–709. <https://doi.org/10.1016/j.apsusc.2016.01.262>
22. Lozano GE, Beatriz SR, Cervantes FM, María GNP, Francisco JMC. Low accuracy of the McFarland method for estimation of bacterial populations. *African J Microbiol Res*. 2018 August; 12(31): 736–740. <https://doi.org/10.5897/AJMR2018.8893>
23. Rasmussen MK, Pedersen JN, Marie R. Size and surface charge characterization of nanoparticles with a salt gradient. *Nat Commun*. 2020 December; 11(1): 2337. <https://doi.org/10.1038/s41467-020-15889-3>
24. Faried M, Shameli K, Ubaidillah, Miyake M, Hara H, Khairudin NBA. Green synthesis of silver nanoparticles in biopolymer stabilizer and their application as antibacterial efficacy. *AIP Conf Proc*. 2017 January; 1788(1): 30124. <https://doi.org/10.1063/1.4968377>
25. Yerragopu PS, Hiregoudar S, Nidoni U, Ramappa KT, Sreenivas AG, Doddagoudar SR. Chemical Synthesis of Silver Nanoparticles Using Tri-sodium Citrate, Stability Study and Their Characterization. *Int Res J Pure Appl Chem*. 2020 March; 21(3): 37–50. <https://doi.org/10.9734/irjpac/2020/v21i330159>
26. Liu F, Ma D, Luo X, Zhang Z, He L, Gao Y, et al. Fabrication and characterization of protein-phenolic conjugate nanoparticles for co-delivery of curcumin and resveratrol. *Food Hydrocoll*. 2018 June; 79: 450–461. <https://doi.org/10.1016/j.foodhyd.2018.01.017>
27. Zhang JZ. *Optical properties and spectroscopy of nanomaterials*. Singapore: World Scientific; 2009. 400 p.
28. Figueiredo NM, Cavaleiro A. Dielectric Properties of Shape-Distributed Ellipsoidal Particle Systems. *Plasmonics*. 2020 April; 15(2): 379–397. <https://doi.org/10.1007/s11468-019-01051-3>
29. Samson D, Adeeko T, Makama E. Synthesis and optical characterization of silver nanoparticles (Ag-NPs) thin films (TFs) prepared by silar technique. *Int J Curr Res Acad Rev*. 2017 December; 5(12): 15–24. <https://doi.org/10.20546/ijcrar.2017.512.003>
30. Sharma S, Yadava DK, Chawla K, Lala N, Jaine PK, Kumar S, et al. Synthesis and Characterization of Silver Nanoparticles by *Murraya Koenigii* Leaves. *J Kejuruter*. 2022 January; 34(5): 819–824. [https://doi.org/10.17576/jkukm-2022-34\(5\)-07](https://doi.org/10.17576/jkukm-2022-34(5)-07)
31. Majeed Khan MA, Kumar S, Ahamed M, Alrokayan SA, Alsalhi MS. Structural and thermal studies of silver nanoparticles and electrical transport study of their thin films. *Nanoscale Res Lett*. 2011 June; 6(1): 434. <https://doi.org/10.1186/1556-276X-6-434>
32. Yildiz A, Cansizoglu H, Abdulrahman R, Karabacak T. Effect of grain size and strain on the bandgap of glancing angle deposited AZO nanostructures. *J Mater Sci Mater Electron*. 2015 August; 26(8): 5952–5957. <https://doi.org/10.1007/s10854-015-3167-0>
33. Wilson WW, Wade MM, Holman SC, Champlin FR. Status of methods for assessing bacterial cell surface charge properties based on zeta potential measurements. *J Microbiol Methods*. 2001 January; 43(3): 153–164. [https://doi.org/10.1016/S0167-7012\(00\)00224-4](https://doi.org/10.1016/S0167-7012(00)00224-4)
34. Lunardi CN, Gomes AJ, Rocha FS, De Tommaso J, Patience GS. Experimental methods in chemical engineering: Zeta potential. *Can J Chem Eng*. 2021 March; 99(3): 627–639. <https://doi.org/10.1002/cjce.23914>
35. Ahmad SA, Das SS, Khatoun A, Ansari MT, Afzal M, Hasnain MS, et al. Bactericidal activity of silver nanoparticles: A mechanistic review. *Mater Sci Energy Technol*. 2020 January; 3(1): 756–769. <https://doi.org/10.1016/j.mset.2020.09.002>
36. Hasson SO, Salman SAK, Hassan SF, Abbas SM. Antimicrobial Effect of Eco-Friendly Silver Nanoparticles Synthesis by Iraqi Date Palm (*Phoenix dactylifera*) on Gram-Negative Biofilm-Forming Bacteria. *Baghdad Sci J*. 2021 December; 18(4): 1149–1156. <https://doi.org/10.21123/bsj.2021.18.4.1149>
37. Ameh T, Gibb M, Stevens D, Pradhan SH, Braswell E, Sayes CM. Silver and Copper Nanoparticles Induce Oxidative Stress in Bacteria and Mammalian Cells. *Nanomaterials*. 2022 July; 12(14): 2402. <https://doi.org/10.3390/nano12142402>
38. Kambale EK, Nkanga CI, Mutonkole B-PI, Bapolisi AM, Tassa DO, Liesse J-MI, et al. Green synthesis of antimicrobial silver nanoparticles using aqueous leaf extracts from three Congolese plant species (*Brillantaisia patula*, *Crossopteryx febrifuga* and *Senna siamea*). *Heliyon*. 2020 August; 6(8): e04493. <https://doi.org/10.1016/j.heliyon.2020.e04493>
39. Urnukhsaikhan E, Bold B-E, Gunbileg A, Sukhbaatar N, Mishig-Ochir T. Antibacterial activity and characteristics of silver nanoparticles biosynthesized from *Carduus crispus*. *Sci Rep*. 2021 December; 11(1): 21047. <https://doi.org/10.1038/s41598-021-00520-2>

## تحضير ودراسة خواص جسيمات الفضة النانوية و تطبيقاتها الطبية ضد البكتيريا المرضية

ذكري عبد الوهاب مصطفى<sup>2</sup>

روژه برهان الدين عبدالرحمن<sup>1</sup>

نه زين زينل عباس<sup>1</sup>

<sup>1</sup> قسم الفيزياء، كلية العلوم، جامعة كركوك، كركوك، العراق.

<sup>2</sup> كلية الطب البشري، جامعة كركوك، كركوك، العراق.

### الخلاصة:

في هذه الدراسة تم تصنيع جسيمات الفضة النانوية (Ag NPs) الصلدة والجوفاء تم توصيف الجسيمات النانوية باستخدام المجهر الإلكتروني النافذ (TEM)، وجهد زيتا، والتحليل الطيفي للأشعة المرئية وال فوق البنفسجية، و حيود الأشعة السينية (XRD). كشفت صورة TEM عن شكل الشبه الكروي لكل من جسيمات الفضة النانوية (Ag NPs) الصلدة والجوفاء. كشف قياس الشحنة السطحية أنه جسيمات الفضة النانوية الجوفاء (Hollow Ag NPs) لها شحنة سطحية تبلغ قيمتها 43- مللي فولت، بينما جسيمات الفضة النانوية الصلدة (Solid Ag NPs) لها شحنة سطحية تبلغ قيمتها 33- مللي فولت. أظهرت جسيمات الفضة النانوية الصلدة والجوفاء قمم امتصاص عند أطوال موجية 436 نانومتر و 412 نانومتر، على التوالي، وفقاً لقياس التحليل الطيفي للأشعة فوق البنفسجية. اظهرت نتائج حيود الأشعة السينية أن التركيب البلوري للعينات مكعب وبأحجام جسيمات تبلغ حوالي 28 نانومتر و 27 نانومتر لجسيمات الفضة النانوية الصلدة والجوفاء، على التوالي. تم اختبار النشاط المضاد للميكروبات من Ag NPs المحضر على بعض السلالات البكتيرية الممرضة التي تم عزلها من مرضى التهاب المسالك البولية (UTI). والحروق , أظهرت نتائج التجربة فعالية إيجابية مبيده للجراثيم ضد البكتيريا المعزولة وكانت جسيمات الفضة النانوية الصلدة أكثر فاعلية ضد بكتيريا G-ve و G + ve. بالإضافة الى ان النشاط المضاد للميكروبات للجسيمات النانوية الصلدة كان معتمد على الوقت و التركيز.

**الكلمات المفتاحية:** جسيمات الفضة النانوية، مضاد بكتيري، البنية النانوية، TEM، جهد زيتا.